Ab initio molecular-dynamics simulations of liquid GaSb and InSb

Tingkun Gu,[1,2] Xiufang Bian,[1] Jingyu Qin,[1] and Changye Xu[3]
[1]*The Key Laboratory of Liquid Structure and Heredity of Materials, Ministry of Education, Shandong University—Southern Campus, Jinan 250061, People's Republic of China*
[2]*School of Electrical and Engineering, Shandong University, Jinan 250061, People's Republic of China*
[3]*School of Physics and Microelectronics, Shandong University, Jinan 250061, People's Republic of China*
(Received 23 June 2004; revised manuscript received 25 October 2004; published 31 March 2005)

We report results for the structural, dynamical, and electronic properties of liquid GaSb (*l*-GaSb) and liquid InSb (*l*-InSb) simulated by using *ab initio* molecular dynamics. Our calculated structure factors and pair correlation functions for *l*-GaSb and *l*-InSb are in good agreement with available experimental data. The calculated results indicate that covalent heteroatomic bonds similar to those of the crystalline phase are preserved in the liquid state, and the local structures of Ga (In) and Sb atoms in *l*-GaSb and *l*-InSb are analogous with those in pure-element liquids.

DOI: 10.1103/PhysRevB.71.104206 PACS number(s): 71.22.+i

I. INTRODUCTION

The III-V semiconductors have ionic character in chemical bonding compared to group-IV semiconductors. In the crystalline phases of GaSb (*c*-GaSb) and InSb (*c*-InSb), the Ga–Sb and In–Sb bonds have a weak ionic nature, and their Phillips ionicities are 0.261 and 0.31, respectively.[1] Zinc-blende-type GaSb and InSb crystalline phases are stable at ambient conditions with a coordination number of 4. Upon melting, GaSb and InSb become metallic, similar to Si and Ge, and transform to a more close-packed structure with density increases of 8.2% and 12.5%,[2] some of the covalent bonds are broken by the thermal motion of atoms, and the electronic states transform to delocalized or collective states in which compositional defects or "wrong" bonds exist (bonds between the same type of atoms are absent in the crystalline state). Despite the metallic behavior of GaSb and InSb in the melts, they do not have entirely free-electron character, but retain some covalent properties.[3]

Many abnormal phenomena in physical properties of liquid GaSb (*l*-GaSb) and liquid InSb (*l*-InSb) have been reported. For example, the temperature coefficient of resistivity (TCR) has a turning point at 1059 K for *l*-GaSb and 890 K for *l*-InSb.[4] This phenomenon has already been observed for many liquid-Sb-based alloys on the Sb-rich side, and it shows more obviously with increasing Sb content.[5–8] For pure *l*-Ga and *l*-In, the curve of TCR versus temperature is constant over the whole temperature range.[4] But for *l*-Sb, this curve shows a turning point interpreted as a weak Perierls distortion surviving in liquid Sb.[4] Therefore, the abnormal changes observed in the TCR of liquid-Sb-based alloys should be related to the peculiar local structure of Sb atoms in these liquid alloys. The viscosities of *l*-GaSb and *l*-InSb, which were measured by Glazov *et al.*,[3] show non-Arrhenius-type behavior. Kakimoto and Hibiya[9] also measured the viscosities of *l*-GaSb from the melting point to about 1700 K and observed non-Arrhenius-type behavior. A non-Arrhenius relation means that there is not only one regime where the activation behavior can be observed. These experimental results suggest that the liquid structures of GaSb and InSb may change nontrivially with increasing temperature. Although both Glazov *et al.* and Kakimoto and Hibiya used an oscillating viscometer and reported non-Arrhenius-type behavior for *l*-GaSb, the tendencies of the temperature dependence of the viscosity reported by them are inconsistent with each other. Recently, Sato *et al.*[10] measured the viscosities of *l*-GaSb and *l*-InSb by using an improved oscillating viscometer and found a good Arrhenius relationship in the temperature ranges of 991.9–1487.9 K for *l*-GaSb and 779.6–1339.0 K for *l*-InSb. However, they did not measure these viscosities at much higher temperature.

Generally, there are close relations between physical properties and liquid structures. To explain the abnormal change of viscosity versus temperature of *l*-GaSb, Mizuki *et al.*[11] measured the liquid structure of GaSb by neutron diffraction from 1073 to 1323 K, but no obvious changes of total structure factors and pair correlation functions were observed over this temperature range. They used the β-Sn model to explain this experimental phenomenon. But the latest research indicates that the β-Sn model is not suitable to simulate the liquid structure of GaSb alloy.[12] Recently, Wang *et al.*[13] investigated the structures of liquid GaSb and InSb with the extended x-ray-absorption fine-structure method and suggested that covalent heteroatomic bonds should be preserved in the liquid state. It is difficult to determine the partial structure factors of multicomponent liquids by experiment. For example, in order to get the three partial structure factors of a liquid binary alloy, researchers generally combine x-ray diffraction and neutron scattering in which isotopic substitution has to be used. Neutron scattering experiments on liquid metals are costly because of the special instruments needed for high temperature and limited neutron sources. Moreover, to get more accurate partial structures, the alloy composition and the isotope type must be carefully selected. So the majority of the experimental data on the structure of molten alloys are published in the form of total structure factors in the literature. Thus, reports of the partial structure factors or partial pair correlation functions of *l*-GaSb and *l*-InSb have not been seen so far. In order to make further investigation of *l*-GaSb and *l*-InSb, the three

TABLE I. The temperatures and densities of *l*-GaSb, *l*-InSb, *l*-Ga, *l*-In, and *l*-Sb used in calculations.

System	*l*-GaSb	*l*-InSb	*l*-Ga	*l*-In	*l*-Sb
Temperature (K)	1073	813	1073	973	933
Density (g cm^{-3})[a]	6.01	6.51	5.61	6.61	6.48

[a]The experimental densities are taken from Sato *et al.* (Ref. 10) for *l*-GaSb and *l*-InSb, and Waseda (Ref. 31) for *l*-Ga, *l*-In, and *l*-Sb.

partial pair correlation functions of these liquids should be measured.

To gain more insight into the structural and dynamical properties and chemical bonding associated with *l*-GaSb and *l*-InSb, we have performed *ab initio* molecular-dynamics (AIMD) simulations. The AIMD simulations are based on density-functional theory[14] (DFT) and the pseudopotential method,[15] following the methods pioneered by Car and Parrinello.[16] DFT is generally accurate for metals and semiconductors, and previous AIMD simulations of liquids, such as Si,[17] Ge,[18] Ga,[19] GaSe,[20] GaAs,[21,22] CdTe,[23] GeTe,[24] etc., have demonstrated close agreement with the experimental results. Molteni *et al.*[25] studied the liquid structure of GaAs and GaSb with tight-binding molecular-dynamics simulations in which the calculated structure factors are in disagreement with the experimental results since the tight-binding simulation has some restrictions (it is not self-consistent and the basis set is limited). In this paper, we will carry out *ab initio* MD simulations for *l*-GaSb and *l*-InSb and focus on studying their structural features, dynamical properties, and electronic structures.

II. COMPUTATIONAL METHODS

Our calculations have been performed by using the Vienna *ab initio* simulation program VASP.[26,27] The first-principles calculations presented here are based on density-functional theory within the generalized gradient approximation (GGA). Our GGA calculations use the PW91 functional due to Perdew and Wang.[28] We use ultrasoft pseudopotentials of Vanderbilt type to describe the electron-ion interaction.[29,30] As the electronic ground state is calculated exactly after each ionic move, the system always remains in the adiabatic ground state, this is an evident advantage in MD simulations for metallic system.

Our simulations for liquid GaSb, InSb, Ga, In, and Sb have been performed with a cubic supercell which contains 80 atoms and periodic boundary conditions are imposed. The used temperatures and experimental densities[10,31] are shown in Table I. The simulations are performed in a canonical ensemble with a Nosé thermostat for temperature control.[32] The equation of motion is solved via the velocity Verlet algorithm with a time step of 3 fs. The Γ point alone is used to sample the Brillouin zone of the supercell. After initial equilibration, we acquire structure information during another 12 ps period in which the energy conservation is excellent and the drift is smaller than 0.5 meV/atom/ps.

III. STRUCTURAL PROPERTIES

In a molecular-dynamics simulation of the liquid state, the structure factor $S(k)$ serves as a connection with the experimental results. $S(k)$ is one of the few experimental data to yield structural information for a semiconductor in the liquid phase. In our paper, the total structure factor is expressed as a linear combination of the partial structural factors $S_{ij}(K)$:

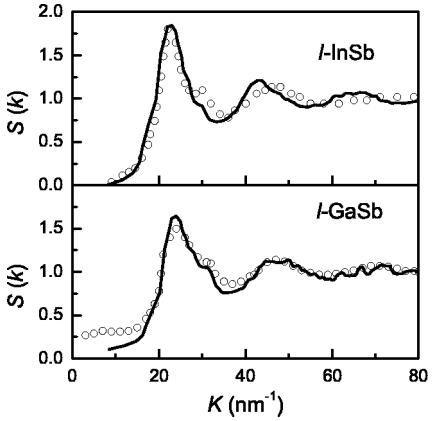

FIG. 1. Calculated total structure factor $S(k)$ of liquid GaSb and InSb (full lines) compared with the result of experiment (circles).

$$S(k) = \sum_i \sum_j c_i^{1/2} c_j^{1/2} \frac{b_i b_j}{c_i b_i^2 + c_j b_j^2} S_{ij}(k), \tag{1}$$

where b_i is the neutron scattering length of the ith species [$b_{Ga}=7.288$ fm,[33] $b_{Sb}=5.25$ fm (Ref. 34)], and c_i is the concentration. For *l*-InSb, the neutron scattering length b_i in Eq. (1) is replaced by the atomic scattering factor $f_i(k)$.

The calculated structure factors are shown in Fig. 1 in which we compare them with the experimental structure factors obtained by neutron diffraction for *l*-GaSb (Ref. 11) and x-ray diffraction for *l*-InSb,[35] respectively. Our calculated structure factors of *l*-GaSb and *l*-InSb are in agreement with experimental results in tendency. The liquid structure of III-V compounds (GaAs and GaSb) was calculated by Molteni *et al.*[25] with a tight-bonding molecular-dynamics simulation in which they failed to reproduce the small shoulder on the right-hand side of the first peak in the structure factors. The presence of the shoulder on the right-hand side of the first peak in $S(k)$ implies a nonsimple local structure in the liquid. On further inspection of the change of the shoulder's intensity from metallic to covalent liquids in the fourth-row elements, it first appears in liquid Ge and intensifies in the less metallic liquid Si and is absent in liquid Pb and Sn.[36] Thus, this shoulder appears to be a signature of local order resulting from covalent bonding in the liquid.

Better insight into the liquid structure is provided by the pair correlation function $g(r)$. The total pair correlation functions of *l*-GaSb and *l*-InSb obtained by weighting the partial pair correlation function with the neutron scattering length (or atomic scattering factor for *l*-InSb) are shown in Fig. 2. The calculated total pair correlation function of *l*-GaSb is in good agreement with the experimental result[11] in which the small peak at 0.2 nm is artificial, arising from the limited k range of the experimental structure factor [the experimental pair correlation function is calculated from structure factor $S(k)$ by Fourier transform]. Given the pair correlation func-

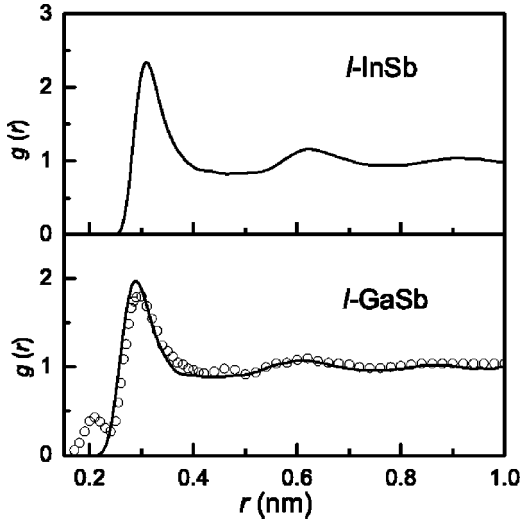

FIG. 2. Calculated total pair correlation function $g(r)$ (full lines) compared with the experimental result (circles, Ref. 11).

tion, it is possible to estimate coordination numbers as in Ref 11:

$$N = 2\int_0^{r_{\max}} 4\pi r^2 \rho g(r) dr, \tag{2}$$

where $r_{\max}$ is the position of the first peak in radial distribution function $4\pi r^2 \rho g(r)$. (For *l*-GaSb, $r_{\max}=0.295$ nm. For *l*-InSb, $r_{\max}=0.31$ nm.) We find $N=5.5$ for *l*-GaSb and its corresponding experimental value is 5.4 ± 0.5.[11] In case of *l*-InSb, the coordination number is 5.6.

The calculated partial pair correlation functions of *l*-GaSb and *l*-InSb are shown in Fig. 3. To investigate the character of the correlations between the same types of atoms, the calculated pair correlation functions of pure *l*-Ga, *l*-In, and *l*-Sb, which are all in good agreement with the

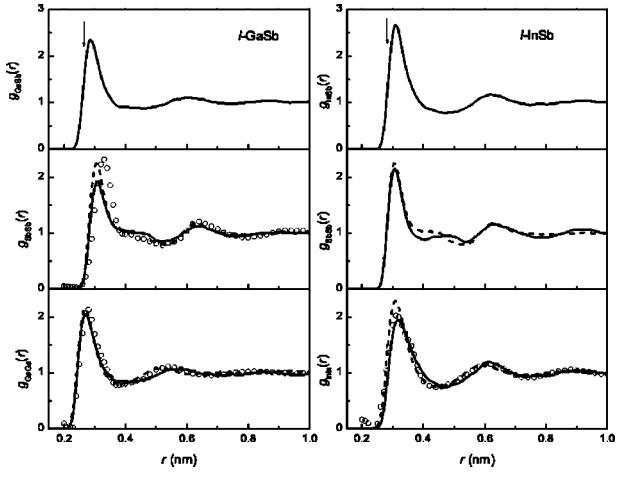

FIG. 3. The calculated partial pair correlation functions of *l*-GaSb and *l*-InSb (full lines), and the pair correlation functions of *l*-Ga, *l*-In, and *l*-Sb. Dash lines, *ab initio* MD; circles, x-ray diffraction of Waseda (Ref. 31). The vertical arrow denotes the nearest-neighbor distance of Ga–Sb and In–Sb in the crystalline states.

TABLE II. Partial coordination numbers and nearest-neighbor distances (in nm) for *l*-GaSb and *l*-InSb (α=Ga or In, β=Sb).

System	$N_{\alpha\alpha}/r_{\alpha\alpha}$	$N_{\alpha\beta}/r_{\alpha\beta}$	$N_{\beta\beta}/r_{\beta\beta}$	CDN
l-GaSb	2.2/0.28	2.5/0.29	1.7/0.305	0.78
l-InSb	1.7/0.315	2.5/0.31	1.6/0.305	0.66

experimental results,[31] are also shown in this figure. The pair correlation functions of *l*-Ga and *l*-In have a well-defined first shell. But for *l*-Sb, its pair correlation function is more complex with a small shoulder on the right-hand side of the main peak. The previous *ab initio* calculation[37] and experimental result[38] indicate that there are covalent bonds surviving in *l*-Sb near the melting point.

It can be seen that there is a certain difference between the local structures of Ga–Ga and Sb–Sb for *l*-GaSb. For Sb–Sb, the overall features of $g_{\mathrm{SbSb}}(r)$ in *l*-GaSb resembles those in *l*-Sb including the same positions of the first and second peaks as well as the small shoulder on the right-hand side of the main peak. The only difference between them is that the first peak of $g_{\mathrm{SbSb}}(r)$ in *l*-GaSb is lower than that in *l*-Sb. In the case of Ga–Ga, there are well-defined first and second peaks in $g_{\mathrm{GaGa}}(r)$, while for liquid GaAs the second peak of $g_{\mathrm{GaGa}}(r)$ disappears.[21] Except for the slightly lower first peak, the $g_{\mathrm{GaGa}}(r)$ of *l*-GaSb is also similar to that in *l* -Ga.

For *l*-InSb, the first peak height of $g_{\mathrm{InSb}}(r)$ is also higher than those of $g_{\mathrm{InIn}}(r)$ and $g_{\mathrm{SbSb}}(r)$ as in *l*-GaSb. There are also some differences between the local structures of In–In and Sb–Sb in *l*-InSb instanced by the first peak of $g_{\mathrm{SbSb}}(r)$ being sharper than that of $g_{\mathrm{InIn}}(r)$. We find that the overall features of $g_{\mathrm{InIn}}(r)$ and $g_{\mathrm{SbSb}}(r)$ in *l*-InSb are slightly different from those in *l*-In and *l*-Sb, respectively. The first peak of $g_{\mathrm{SbSb}}(r)$ of *l*-InSb almost overlaps with that of *l*-Sb, but the small shoulder on the right-hand side of the main peak of $g(r)$ in *l*-Sb shows as a small peak in *l*-InSb. The first peak of $g_{\mathrm{InIn}}(r)$ in *l*-InSb becomes broader than that in *l*-In.

Given the partial pair correlation functions, it is possible to calculate the partial coordination numbers as

$$N_{\alpha\beta} = 2\int_0^{R_{\max}} 4\pi r^2 \rho_\beta g_{\alpha\beta}(r) dr, \tag{3}$$

where $R_{\max}$ is the first maximum coordinate (the nearest-neighbor distance) in $4\pi r^2 \rho_\beta g_{\alpha\beta}(r)$. The nearest-neighbor distances and the calculated partial coordination numbers of *l*-GaSb and *l*-InSb are illustrated in Table II. To estimate the compositional defects, a compositional disorder number (CDN), defined as the ratio of homogeneous and heterogeneous bonds $(N_{\alpha\alpha}+N_{\beta\beta})/2N_{\alpha\beta}$ is calculated and also illustrated in Table II. We find that both the compositional disorder numbers of *l*-GaSb and *l*-InSb are smaller than 1. This indicates that the atoms are likely to have neighbors of different type species in *l*-GaSb and *l*-InSb.

The bond-angle distributions of the same type atoms are presented in Fig. 4. The functions are defined as the average of angles between a reference atom and all pairs of the same

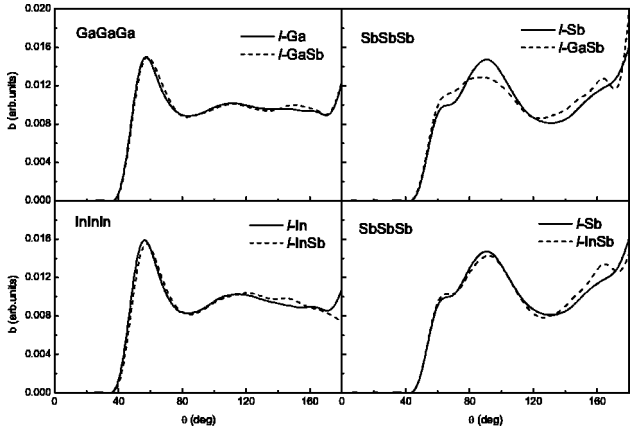

FIG. 4. Bond-angle distributions of Ga, In, and Sb atoms. The cutoff distances of b_{GaGaGa}, b_{InInIn}, and b_{SbSbSb}, are 0.36, 0.40, and 0.34 nm, respectively.

type atoms within a cutoff distance r_c of the reference atom. In our calculations, we select the r_c that includes the symmetric part of the first peak of the partial correlation function. To emphasize the deviation from random distributions, bond-angle distributions are normalized by $\sin(\theta)$. Both the b_{GaGaGa} of *l*-GaSb and b_{InInIn} of *l*-InSb have two peaks near 60° and 120°. Such peaks are expected in close-packed liquids, and are also found in pure *l*-Ga (Ref. 19) and *l*-In. The first peaks of b_{GaGaGa} and b_{InInIn} in *l*-GaSb and *l*-InSb are in good coincidence with those in *l*-Ga and *l*-In. Both the b_{SbSbSb} of *l*-GaSb and *l*-InSb have two peaks at ~90° and ~180°. Seifert *et al.*[37] also studied the structure of pure *l*-Sb, and found these two peaks in which they indicated that a weak Peierls distortion exists in *l*-Sb as its crystalline state. Thus, the local structures of Sb in *l*-GaSb and *l*-InSb are similar to that in *l*-Sb. As compared with *l*-Sb, the b_{SbSbSb} of *l*-GaSb has a lower first peak and a higher second peak, and its first peak shifts to smaller angle, while the b_{SbSbSb} of *l*-InSb is almost identical with that of *l*-Sb.

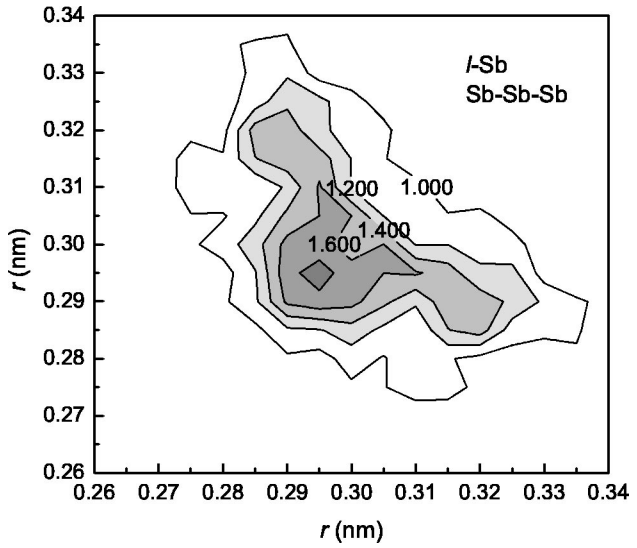

FIG. 5. Angular limited triplet correlation function $P(r_1, r_2)$ of *l*-Sb.

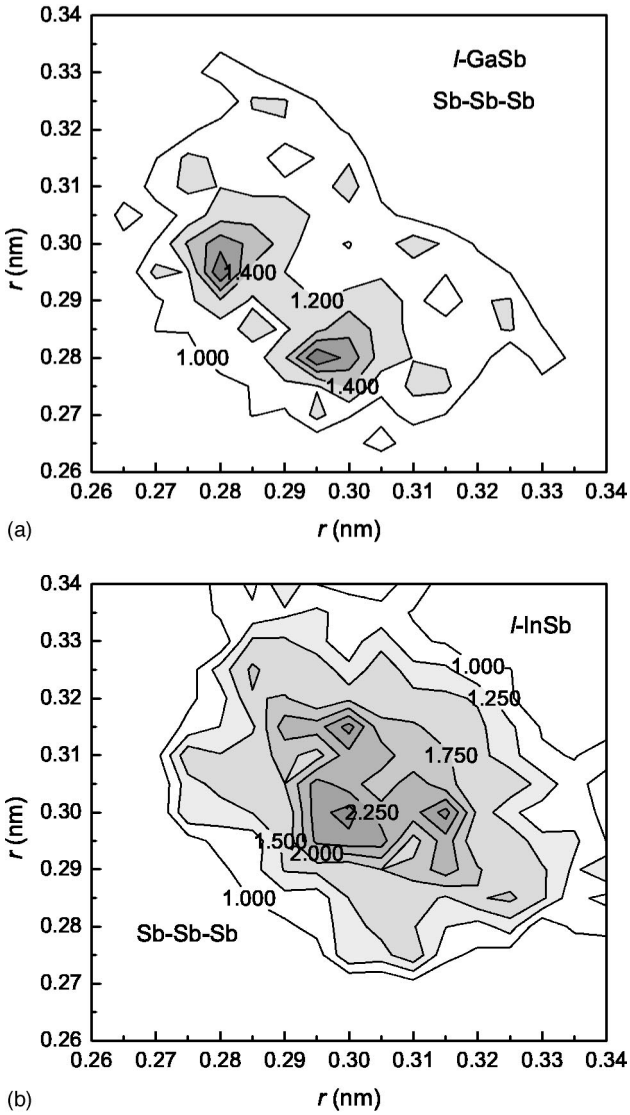

FIG. 6. Angular limited triplet correlation functions $P(r_1, r_2)$ of *l*-GaSb and *l*-InSb.

To investigate the peak around 180° of b_{SbSbSb} of *l*-GaSb and *l*-InSb in detail, we calculate the angular limited triplet correlation function of Sb−Sb−Sb in *l*-Sb, *l*-GaSb, and *l*-InSb, which are plotted in Figs. 5 and 6. This function $P(r_1, r_2)$ is defined as the probability of finding an atom *C* at a distance r_2 from an atom *B*, which is at a distance r_1 from the reference atom *A*. A constraint is placed on the position of atom *C*; namely, the *BC* bond is constrained in a cone of small angular aperture (here, 20°) around the *AB* axis. For an undistorted disorder structure, the maximum of the distribution should be on the diagonal (i.e., a maximum at $r_1 = r_2$). For *l*-Sb, the maxima of the distribution are located at (0.295 nm, 0.295 nm) and the other two strong correlation regions are central at (0.29 nm, 0.32 nm) and (0.32 nm, 0.29 nm). This indicates that the weak Peierls distortion exists in *l*-Sb. From Fig. 6, we find that for *l*-GaSb an obvious correlation appears: a short bond of length r_1 (0.28 nm) is most probably followed by a longer bond of length r_2 (0.30 nm), and vice versa. For *l*-InSb, there are

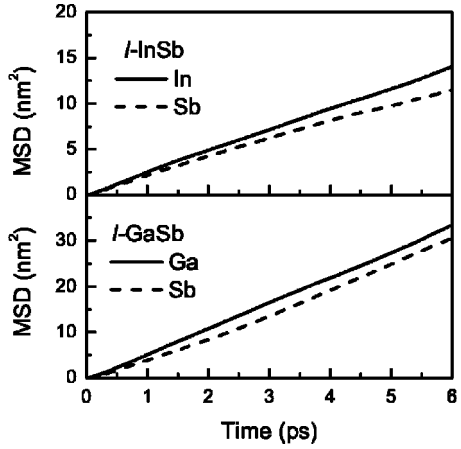

FIG. 7. The time dependence of the mean square displacement of atoms in *l*-GaSb and *l*-InSb.

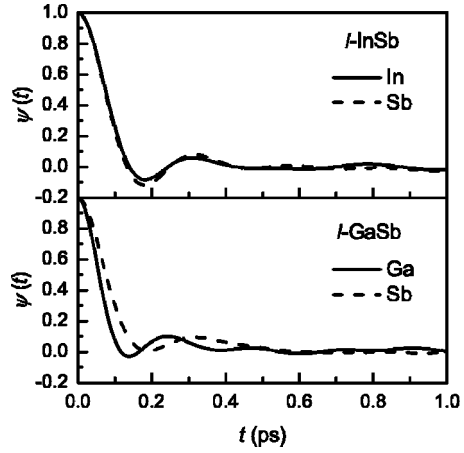

FIG. 8. Velocity autocorrelation functions of *l*-GaSb and *l*-InSb.

three maxima of probability $P(r_1, r_2)$. One is at (0.30 nm, 0.30 nm), and the other two at (0.30 nm, 0.315 nm) and (0.315 nm, 0.30 nm), respectively. Although there are several differences of local structure for Sb atoms between *l*-GaSb, and *l*-InSb, they have a common feature in which a correlation between the short and long bonds for Sb atoms as in *l*-Sb.

IV. DYNAMICAL PROPERTIES

In Fig. 7, we illustrate the mean-square displacements as a function of time for *l*-GaSb and *l*-InSb. The calculated diffusion coefficients are shown in Table III. Unfortunately, there appear to be no experimental data for the diffusion coefficients of *l*-GaSb and *l*-InSb. To verify the calculated results, we calculate the viscosities of *l*-GaSb and *l*-InSb by using their relationships with the diffusion coefficients calculated by the Stokes-Einstein relation:[39]

$$\eta = \frac{k_B T}{2\pi a D}, \tag{4}$$

where $D = (D_{\mathrm{Ga(In)}} + D_{\mathrm{Sb}})/2$, and a is the effective "diameter" of the diffusing particles. We define the particle size a as the average value of the nearest-neighbor distances of Ga–Ga (In–In) and Sb–Sb in *l*-GaSb and *l*-InSb (0.29 nm for *l*-GaSb and 0.31 nm for *l*-InSb). The calculated viscosities of *l*-GaSb and *l*-InSb are in good agreement the experimental results.[3,9,10]

TABLE III. Diffusion coefficients (in 10^{-5} cm^{-2}/s) for Ga(In) and Sb atoms and viscosities (in mPa s) of *l*-GaSb and *l*-InSb. Values in parentheses show the diffusion coefficients obtained from Eq. (7).

System	T	$D_{\mathrm{Ga(In)}}$	D_{Sb}	η^{a}	η^{b}
l-GaSb	1073	9.32 (9.39)	8.72 (8.56)	0.90	0.87
l-InSb	813	4.03 (4.02)	3.45 (3.66)	1.54	1.14

[a]This work.
[b]The experimental results (Ref. 10).

More detailed information about the single-particle dynamics can be obtained by studying the velocity autocorrelation function $\psi(t)$ defined as[40]

$$\psi(t) = \frac{\langle \mathbf{V}_i(0) \cdot \mathbf{V}_i(t) \rangle}{\langle \mathbf{V}_i(0) \cdot \mathbf{V}_i(0) \rangle}, \tag{5}$$

where $\boldsymbol{V}_i(t)$ is the velocity of particle i and $\langle \cdots \rangle$ denote an average over particles and over time origins. The corresponding spectral density $Z(\nu)$ is given by

$$Z(\nu) = \int_0^\infty \psi(t) \cos(\nu t) dt. \tag{6}$$

The two functions for each atomic species are shown in Figs. 8 and 9. Shoulders of $Z(\nu)$ occur at about 2.5 THz for Ga and Sb atoms in *l*-GaSb and 3.0 THz for In and Sb atoms in *l*-InSb. In the crystalline states, the optical phonon peak is at about 7 THz for GaSb and 6 THz for InSb at 300 K. It will shift to lower values as the temperature rises.

The diffusion coefficients can also be calculated by using the relation

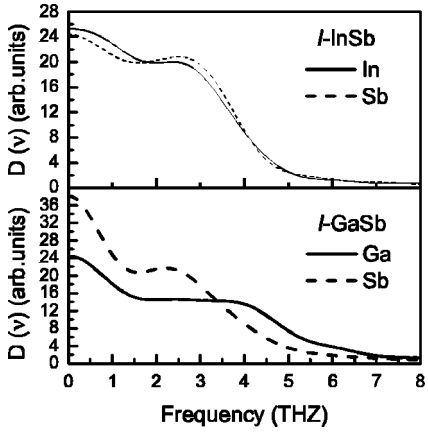

FIG. 9. Spectral densities of *l*-GaSb and *l*-InSb.

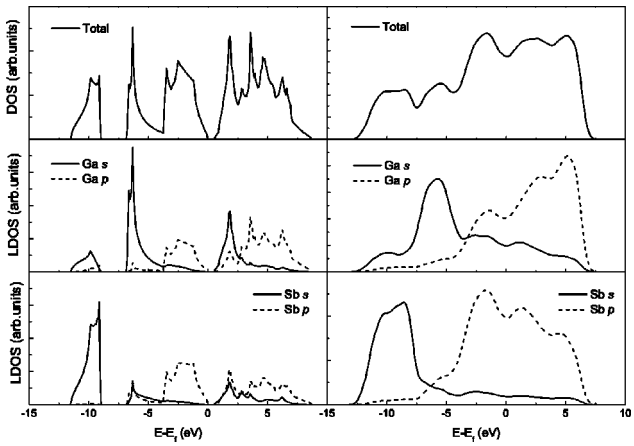

FIG. 10. Total electronic density of states and the local density of states for GaSb in zinc-blende structure (left panel) and liquid structure (right panel).

$$D = \frac{k_B T}{M} \int_0^\infty Z(t)dt = \frac{k_B T}{M} Z(0). \tag{7}$$

The data derived by Eq. (7) are really close to the data calculated from MSD.

V. ELECTRONIC STRUCTURE

The structural behavior of liquid alloys can be understood in terms of the electronic structure. Here we have investigated the electronic density of states (DOS) and the local density of states (LDOS).[41] The LDOSs are obtained by projecting the wave functions onto spherical harmonics centered on each atom with a radius of 0.144 nm for In atoms, 0.128 nm for Ga atoms, and 0.14 nm for Sb atoms (covalent radius). Both the DOS and LDOS are obtained by averaging on ten configurations.

The DOS and LDOS for *l*-GaSb and *c*-GaSb (zinc-blende structure) as well as *l*-InSb and *c*-InSb are shown in Figs. 10 and 11, respectively. It is instructive to investigate the character of the DOS and LDOS in the liquid and crystalline states. In the zinc-blende structure, a gap at the Fermi level as a signature of a semiconductor is observed, a sharpening of both the *s* and *p* peaks for Ga, In, and Sb atoms can be found, and there are complete overlaps between the two *p* states which contribute to the heteroatomic bonds. In the liquid state, the gap at the Fermi level disappears, demonstrating metalliclike behavior, but a small "dip" still exists. There is a broadening of the *s* and *p* levels for Ga, In, and Sb atoms and less overlap between the two *p* states of the different type atoms. Some similarities of the DOS and LDOS of the liquids to those of crystalline states are also visible. For instance, the peak positions of Ga *s*, In *s*, and Sb *s* states in *l*-GaSb and *l*-InSb are the same as in the crystalline states, and the overlaps of the LDOS between Ga (In) and Sb atoms mainly resulting from the two *p* states in liquids are similar to those in the crystalline states.

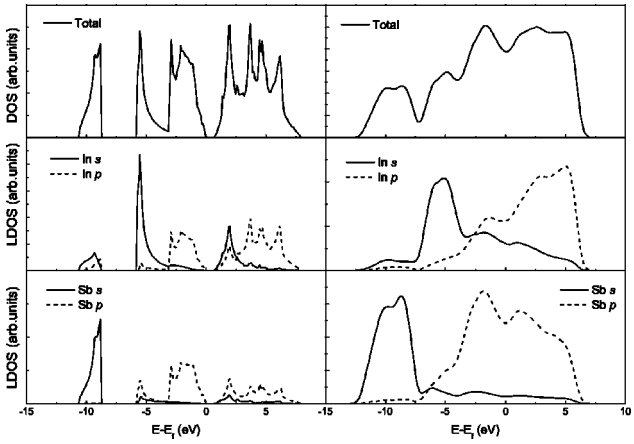

FIG. 11. Total electronic density of states and the local density of states for InSb in zinc-blende structure (left panel) and liquid structure (right panel).

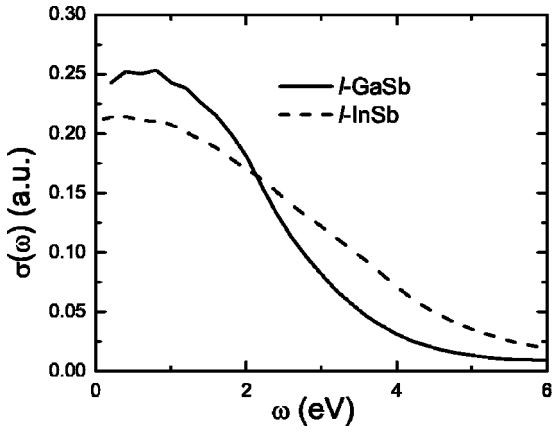

FIG. 12. Real part of optical conductivities of *l*-GaSb and *l*-InSb.

Once the energy states and wave functions for a given atomic configuration are obtained, the optical conductivity can be calculated by using the Kubo-Greenwood expression.[42] The real part of the conductivity is determined by the sum of all possible dipole transition at a given frequency:

$$\sigma(\omega) = \frac{2\pi e^2}{3m^2\omega\Omega} \sum_m^{\text{occ}} \sum_n^{\text{unocc}} \sum_{\alpha=x,y,z} |\langle \psi_m | p_\alpha | \psi_n \rangle|^2 \delta(E_n - E_m - \hbar\omega) \tag{8}$$

where E_i and ψ_i are the eigenvalues and eigenfunctions, and Ω is the volume of the supercell. The calculated conductivities are illustrated in Fig. 12. They show a Drude-like falloff. This behavior has also been found in *l*-Si, *l*-Ge, and *l*-GaAs as a signature of a metallic liquid.[17,18,22] We can extrapolate the frequency-dependent conductivity to zero frequency to estimate the dc conductivity. The estimated value $\sim 10\,500\ \Omega^{-1}\,\text{cm}^{-1}$ for *l*-GaSb and $\sim 9660\ \Omega^{-1}\,\text{cm}^{-1}$ for *l*-InSb are in remarkable agreement with the experimental values of 10 000–11 400 and 92 000–9900 $\Omega^{-1}\,\text{cm}^{-1}$,[4] respectively. However, considering the several approximations in our calculation, such good agreement is to some extent fortuitous.

By fitting a Drude curve

$$\sigma(\omega) = \frac{\sigma(0)}{1 + \omega^2\tau^2} \tag{9}$$

to our data, we extract a relaxation time $\tau^{-1}=2.69$ eV for *l*-GaSb and $\tau^{-1}=2.59$ eV for *l*-InSb. Although no experimental values of τ are available for *l*-GaSb and *l*-InSb, a value of the same order of magnitude, $\tau^{-1}=2.99$ eV, has been measured in *l*-Si.[43] By using these values of τ, and the free-electron expression $l=\hbar k_F\tau/m$ for the mean free path, we find that the ratios of l/a, where a is the nearest-neighbor distance, are 1.6 for *l*-GaSb and 1.5 for *l*-InSb, indicating a strong scattering behavior in *l*-GaSb and *l*-InSb. In *l*-Si the ratio, calculated in a similar way, is slightly larger, i.e., $l/a=1.8$.[17]

VI. SUMMARY AND CONCLUSION

We have performed *ab initio* molecular-dynamics simulations of *l*-GaSb at temperature 1073 K and *l*-InSb at 813 K. Our theoretical results are in good agreement with available experimental data. In agreement with experiment, *l*-GaSb and *l*-InSb have metallic behavior with the coordination numbers ~5.5 and 5.6. The calculated results for the pair correlation functions and the bond-angle distributions indicate that the correlations of Ga–Ga and Sb–Sb in *l*-GaSb, In–In, and Sb–Sb in *l*-InSb are similar to those in pure *l*-Ga, *l*-In, and *l*-Sb, respectively. The partial bond-angle distributions for Ga and In atoms reveal a pronounced peak near 60° corresponding to the close-packed structure. But for Sb, the partial bond-angle distribution has two main peaks near 90° and 180° corresponding to covalent and chainlike structures, and the local structure of Sb atoms in *l*-GaSb and *l*-InSb is similar to that in pure *l*-Sb. The persistence of bonds of Ga–Sb and In–Sb similar to those of the crystal in the liquid state is indicated by the overlaps between the two *p* states of the different type atoms in the liquid state, similar to those of the crystalline states. We have also calculated the diffusion coefficients for Ga, In, and Sb atoms, and the viscosities of *l*-GaSb and *l*-InSb calculated by the Stokes-Einstein relation are in good agreement with the experimental results. Our investigations of the electronic structures show that there is no gap at the Fermi level in the electronic density of states of *l*-GaSb and *l*-InSb, demonstrating metallic behavior. The dc conductivities of *l*-GaSb and *l*-InSb calculated by the Kubo-Greenwood relation are in agreement with the experimental results.

In conclusion, the calculated results indicate that *l*-GaSb and *l*-InSb contain some features of their crystalline phases and pure Ga (or In) and Sb liquids. Therefore, compared with regular liquid metals, the structures of *l*-GaSb and *l*-InSb are complex. The anomalous variations of the resistivities and the viscosities at certain temperatures in *l*-GaSb and *l*-InSb may be due to the remaining peculiar local structure of Sb atoms and the heteroatomic bonds. To understand the observed phenomena, more extensive and accurate investigations of the structural dependence upon temperature of *l*-GaSb and *l*-InSb are needed.

ACKNOWLEDGMENT

This work was supported by the National Natural Science Foundation of China (Project No. 50471052). We also wish to thank the Shandong High Performance Computing Center.

[1] G. Phillips, *Bands and Bonds in Semiconductors* (Academic Press, New York, 1973).
[2] H. P. Mokroskii and A. R. Regel, J. Tech. Phys. **22**, 1282 (1952).
[3] V. M. Glazov, S. N. Chizhevskaya, and N. N. Glagoleva, *Liquid Semiconductors* (Plenum, New York, 1969).
[4] Q. Wang, X. M. Chen, and K. Q. Lu, J. Phys.: Condens. Matter **12**, 5201 (2000).
[5] M. E. Bakkali, J. G. Gasser, and P. Terzieff, Z. Metallkd. **84**, 662 (1993).
[6] S. Ohno, H. Okazaki, and S. Tamaki, J. Phys. Soc. Jpn. **36**, 1133 (1974).
[7] S. Ohno, H. Okazaki, and S. Tamaki, J. Phys. Soc. Jpn. **35**, 1060 (1973).
[8] A. Bath, J. G. Gasser, J. L. Bretonnet, R. Bianchin, and R. Kleim, J. Phys. (Paris), Colloq. **41**, C8-519 (1980).
[9] K. Kakimoto and T. Hibiya, J. Appl. Phys. **66**, 4181 (1989).
[10] Y. Sato, T. Nishizuka, T. Takamizawa, T. Yamamura, and Y. Waseda, Int. J. Thermophys. **23**, 235 (2002).
[11] J. Mizuki, K. Kakimoto, M. Misawa, T. Fukunaga, and N. Watanabe, J. Phys.: Condens. Matter **5**, 3391 (1993).
[12] T. Hattori, K. Tsuji, N. Taga, Y. Takasugi, and T. Mori, Phys. Rev. B **68**, 224106 (2003)
[13] Y. R. Wang, K. Q. Lu, and C. X. Li, Phys. Rev. Lett. **79**, 3664 (1997).
[14] R. O. Jones and O. Gunnarsson, Rev. Mod. Phys. **61**, 689 (1989).
[15] J. C. Phillips, Phys. Rev. **112**, 685 (1958); M. T. Yin and M. L. Cohen, Phys. Rev. B **25**, 7403 (1982).
[16] R. Car and M. Parrinello, Phys. Rev. Lett. **55**, 2471 (1985).
[17] I. Stich, R. Car, and M. Parrinello, Phys. Rev. B **44**, 11 092 (1991).
[18] G. Kresse and J. Hafner, Phys. Rev. B **49**, 14 251 (1994).
[19] J. M. Holender, M. J. Gillan, M. C. Payne, and A. D. Simpson, Phys. Rev. B **52**, 967 (1995).
[20] J. M. Holender and M. J. Gillan, Phys. Rev. B **53**, 4399 (1996).
[21] V. Godlevsky and James R. Chelikowsky, J. Chem. Phys. **109**, 7312 (1998).
[22] Q. M. Zhang, G. Chiarotti, A. Selloni, R. Car, and M. Parrinello, Phys. Rev. B **42**, 5071 (1990).
[23] V. V. Godlevsky, J. J. Derby, and J. R. Chelikowsky, Phys. Rev. Lett. **81**, 4959 (1998).
[24] J. Y. Raty, V. V. Godlevsky, J. P. Gaspard, C. Bichara, M. Bionducci, R. Bellissent, R. Céolin, James R. Chelikowsky, and Ph. Ghosez, Phys. Rev. B **65**, 115205 (2002).
[25] C. Monlteni, L. Colombo, and L. Miglio, J. Phys.: Condens. Matter **6**, 5255 (1994).
[26] G. Kresse and J. Furthmüller, Comput. Mater. Sci. **6**, 15 (1996).

[27] G. Kresse and J. Furthmüller, Phys. Rev. B **54**, 11 169 (1996).
[28] Y. Wang and J. P. Perdew, Phys. Rev. B **44**, 13 298 (1991).
[29] D. Vanderbilt, Phys. Rev. B **41**, 7892 (1990).
[30] G. Kresse and J. Hafner, J. Phys.: Condens. Matter **6**, 8245 (1994).
[31] Y. Waseda, *The Structure of Non-Crystalline Materials; Liquids and Amorphous Solids* (McGraw-Hill, New York, 1980).
[32] S. Nosé, J. Chem. Phys. **81**, 511 (1984).
[33] G. Reiner, W. Waschkowski, and L. Koester, Z. Phys. A **337**, 221 (1990).
[34] L. Koester, K. Knopf, and W. Waschkowski, Z. Phys. A **323**, 359 (1986).
[35] K. Tsuji, T. Hattori, and T. Kinoshita, Japan Synchrotron Radiation Research Institute (JASRI) SPring-8 User Experiment Report (unpublished).
[36] J. Hafner and W. Jank, Phys. Rev. B **45**, 2739 (1992).
[37] K. Seifert, J. Hafner, and G. Kresse, J. Non-Cryst. Solids **205–207**, 871 (1996).
[38] P. Lamparter and S. Steeb, Z. Naturforsch., A: Phys. Sci. **32**, 1021 (1997).
[39] J. P. Hansen and I. R. McDonald, *Theory of Simple Liquids* (Academic, London, 1986).
[40] P. A. Egelstaff, *An Introduction to the Liquid State* (Clarendon, New York, 1992), p. 240.
[41] A. Eichler, J. Furthmüller, and G. Kresse, Surf. Sci. **346**, 300 (1996).
[42] R. Kubo, J. Phys. Soc. Jpn. **12**, 570 (1957); D. Greenwood, Proc. Phys. Soc. London **71**, 585 (1958).
[43] N. F. Mott and E. A. Davis, *Electronic Processes in Non-Crystalline Materials* (Clarendon, Oxford, 1979).